Pergamon

Bioorganic & Medicinal Chemistry 9 (2001) 2565–2570

BIOORGANIC & MEDICINAL CHEMISTRY

Inducible Regulation of the *S. cerevisiae* Cell Cycle Mediated by an RNA Aptamer–Ligand Complex

Dilara Grate† and Charles Wilson*

Department of Biology and Center for the Molecular Biology of RNA, University of California at Santa Cruz, Santa Cruz, CA 95064, USA

Received 16 October 2000; revised 11 December 2000; accepted 13 December 2000

Abstract—Previous studies have shown that the introduction of a ligand-binding RNA (aptamer) into the 5′-UTR of an mRNA can confer regulated expression of both prokaryotic and eukaryotic reporter genes. The current report shows that aptamer insertion into the 5′-UTR of a cyclin transcript in *S. cerevisiae* renders cell-cycle control dependent upon the presence or absence of the target ligand. A malachite green binding motif, defined by an asymmetric internal loop flanked by short RNA helices, was inserted immediately upstream of the CLB2 start codon. Progression through the cell cycle is dramatically slowed and elongated bud morphology develops when tetramethylrosamine (a fluorescent malachite green analogue) is added to the aptamer-containing strain. Quantification of *CLB2* expression at the RNA and protein levels by RT-PCR and Western blot analysis, respectively, demonstrates that the aptamer ligand regulates transcript translatability rather than stability. One-dimensional NMR spectroscopy shows that the malachite green binding aptamer undergoes a dramatic ligand-dependent change in structure with many nucleotides folding to adopt a well-defined conformation. These results are consistent with a model in which translational initiation is blocked by ligand-induced conformational changes in the 5′-UTR. © 2001 Published by Elsevier Science Ltd.

Introduction

Protein translation in eukaryotes usually involves initial binding by the 40S ribosomal subunit to the 5′-cap of a transcript, followed by scanning to the first initiation codon (reviewed in ref 1). Eukaryotic initiation factors (eIFs) pre-associate with the mRNA to disrupt secondary structure in the 5′-UTR and thereby allow subsequent binding and scanning of the 40S subunit.[2] The efficiency of this process can have a dramatic effect on the overall level of protein synthesis and thus it represents a potential mechanism by which gene expression might be artificially regulated.

Werstuck et al. have previously shown that the insertion of an RNA aptamer into the 5′-UTR of a messenger RNA renders the expression of the aptamer carrying gene controlled by the cognate ligand.[3] Short RNA sequences were selected for the ability to bind either antibiotics or dyes from pools of random sequence molecules. By inserting tandem repeats of antibiotic-binding aptamers into plasmids they were able to create *Escherichia coli* strains with a drug resistance phenotype. In a similar vein, aptamers that specifically bind the dyes Hoechst 33258 and Hoechst 33342 were shown to confer regulated expression of β-galactosidase using both in vitro wheat germ translation extracts and transfected mammalian tissue culture cells.

We have sought to expand upon these results by showing that aptamer-mediated translational regulation can be used to control gene expression in other eukaryotes and by attempting to define the mechanism by which aptamer-mediated regulation is achieved. By monitoring effects at both the RNA and protein levels, we are able to show that the in vivo effects of aptamer insertion result from a change in mRNA translatability rather than mRNA stability. Spectroscopic characterization of the aptamer by 1-D NMR indicates that ligand binding is accompanied by a dramatic folding transition from an unfolded state to a unique, well-defined conformation. Together the observations support a model in which ligand-induced folding of the 5′-UTR limits binding by the 40S ribosomal subunit and thus reduces the rate of translational initiation.

*Corresponding author. Tel.: +1-831-459-5126; fax: +1-831-459-3136; e-mail: wilson@biologyu.ucsc.edu
†Current address: Clontech Laboratories, 1020 East Mendow vCircle, Palo Alto, CA 94303, USA.

0968-0896/01/$ - see front matter © 2001 Published by Elsevier Science Ltd.
PII: S0968-0896(01)00031-1

Results

The *CLB2* gene of *S. cerevisiae* encodes one of four B-type cyclins that normally direct the cell cycle transition from G2 to mitosis in budding yeast (reviewed in ref 4). The concentration of B-type cyclins builds gradually throughout the G2 phase of the cell cycle. Once a critical cyclin concentration is reached, mitosis proceeds and cyclin proteins are rapidly degraded. The cyclin genes are functionally redundant and *S. cerevisiae* deleted for CLB1, CLB3, and CLB4 shows no obvious cell-cycle phenotype. In contrast, strains that fail to express all four B-cyclins have an unusually prolonged cell cycle and display a characteristic elongated bud morphology (buds continue to grow axially without switching to isotropic growth). These easily monitored phenotypes and the fact that they are strongly dependent on relatively modest changes in expression levels make the cyclins a convenient model system for developing and studying artificial controls of gene expression.

The aptamer used for insertion into the *CLB2* transcript was originally selected to bind to the chromophore malachite green [Fig. 1(a)], one a family of triphenyl methane dyes widely used for both industrial and pharmaceutical applications.[5–7] Deletion and mutagenesis experiments suggested an asymmetric bulge structure for the aptamer [Fig. 1(c)], a result recently confirmed by X-ray crystallography.[8] While a potential AUG start codon is present within the original aptamer sequence, it can be eliminated by insertion of an additional Watson–Crick base pair in the stem that flanks the aptamer's conserved core without effecting ligand binding. Tetramethylrosamine (TMR), a structural analogue of malachite green [Fig. 1(b)], binds to the aptamer even more tightly that the original ligand (K_d ~40 nM vs 800 nM).[8] Initial control experiments showed that TMR is readily absorbed by yeast, causing cells to become visibly pink after a short exposure.

The MG aptamer sequence was engineered into the *CLB2* gene as described in Methods. Comparison of yeast strains carrying the normal copy of *CLB2* and the aptamer-inserted gene shows that the aptamer alone causes no strong phenotype in terms of either cell morphology (Fig. 2) or growth rate [Fig. 3(a)]. Cells expressing the unmodified version of the *CLB2* gene grow normally and show no change in morphology following addition of 1 μM TMR (Fig. 2). In contrast,

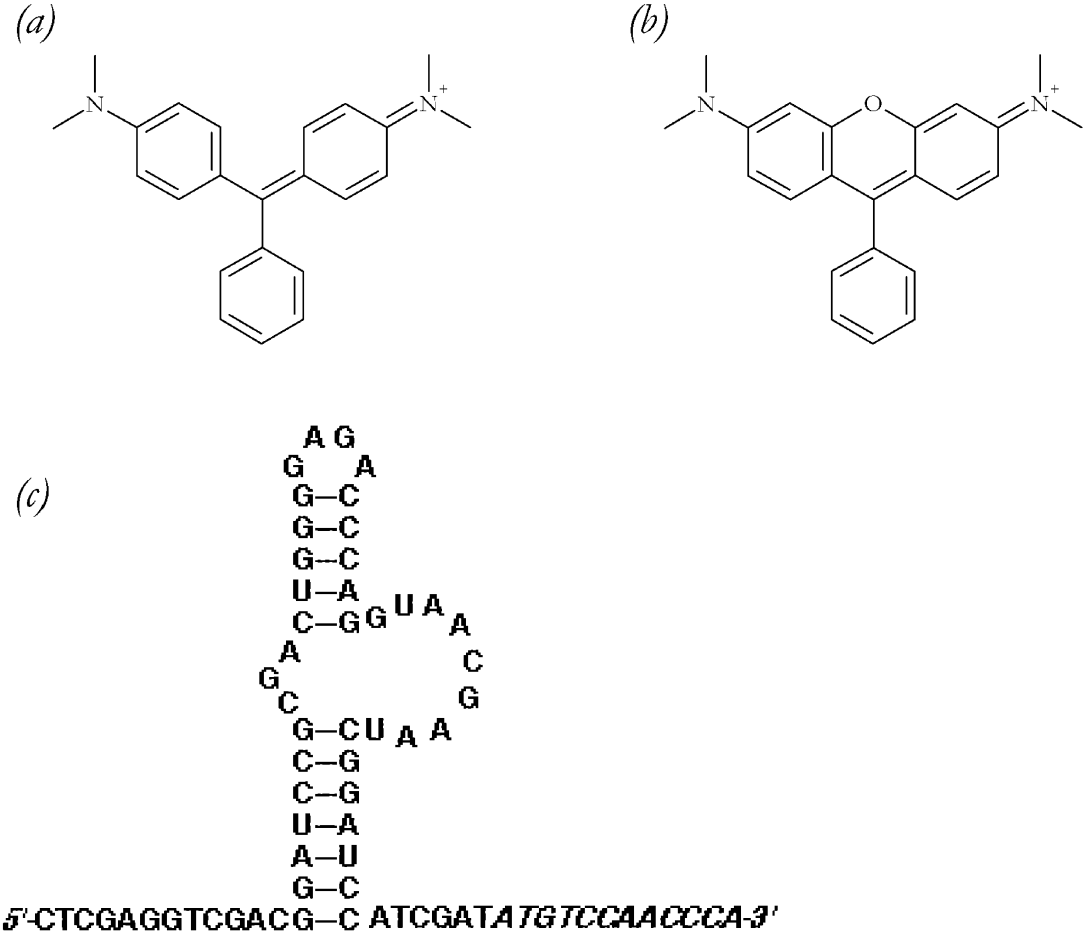

Figure 1. (a) Malachite green (MG) and (b) tetramethylrosamine (TMR) are high-affinity ligands for the in vitro selected MG aptamer. (c) The MG aptamer was engineered into the 5′-UTR of the *Saccharomyces cerevisiae CLB2* gene immediately upstream of the open reading frame (italics) (described in Experimental).

aptamer-bearing cells become highly elongated, forming strings of connected buds, following addition of TMR to their media (Fig. 2). Their growth rate is correspondingly reduced [Fig. 3(a)]. Western analysis of extracts prepared from cells before and after addition of TMR indicates a >10-fold drop in the level of *CLB2* protein [Fig. 3(b)].

The loss of *CLB2* activity could in principle result from a decrease in mRNA concentration or a decrease in mRNA translatability. Elements such as the iron responsive element have been shown to exert either effect depending upon their relative positioning in the mRNA and their juxtaposition with other elements that regulate mRNA stability (e.g., AU-rich elements).[9] To distinguish between these two possibilities, we measured *CLB2* mRNA in the aptamer-tagged strain before and after addition of TMR to the media [Fig. 3(c)]. To reliably quantify the relative *CLB2* transcript concentration, we used an additional pair of primer sets that specifically amplified internal and external standards. A modified *MG-CLB2* standard was prepared by insertion of a 157-bp stuffer sequence into the coding region of the gene. RNA synthesized by in vitro transcription from this template can be amplified using the same primer set as that used for the *MG-CLB2* transcript generated in vivo. By mixing a known amount of the stuffer-containing standard together with total RNA isolated from cells prior to RT-PCR amplification and then comparing the relative intensity of the two amplified products, it is possible to reliably quantitate the amount of the in vivo transcript. CDC42, an endogenous *S. cerevisiae* gene whose transcript concentration does not vary through the cell cycle, was used to monitor the efficiency of mRNA recovery across different samples.[10] As shown in Fig. 3(d), the normalized concentration of the *MG-CLB2* transcript is essentially unaltered by the addition of TMR.

Previous studies of RNA aptamers have shown that ligand binding often induces significant structural changes.[11] The exchangeable imino protons of guanosines and uridines provide a ready means for monitoring such ligand-induced conformational changes by NMR spectroscopy.[12] Generally only those sites involved in internal hydrogen bonding are protected from fast exchange with solvent and thus yield a sharp resonance. Because the imino proton resonances are well separated from the bulk of the RNA resonances (lying at 12–15 ppm), they can be readily identified and interpreted in 1-D spectra.

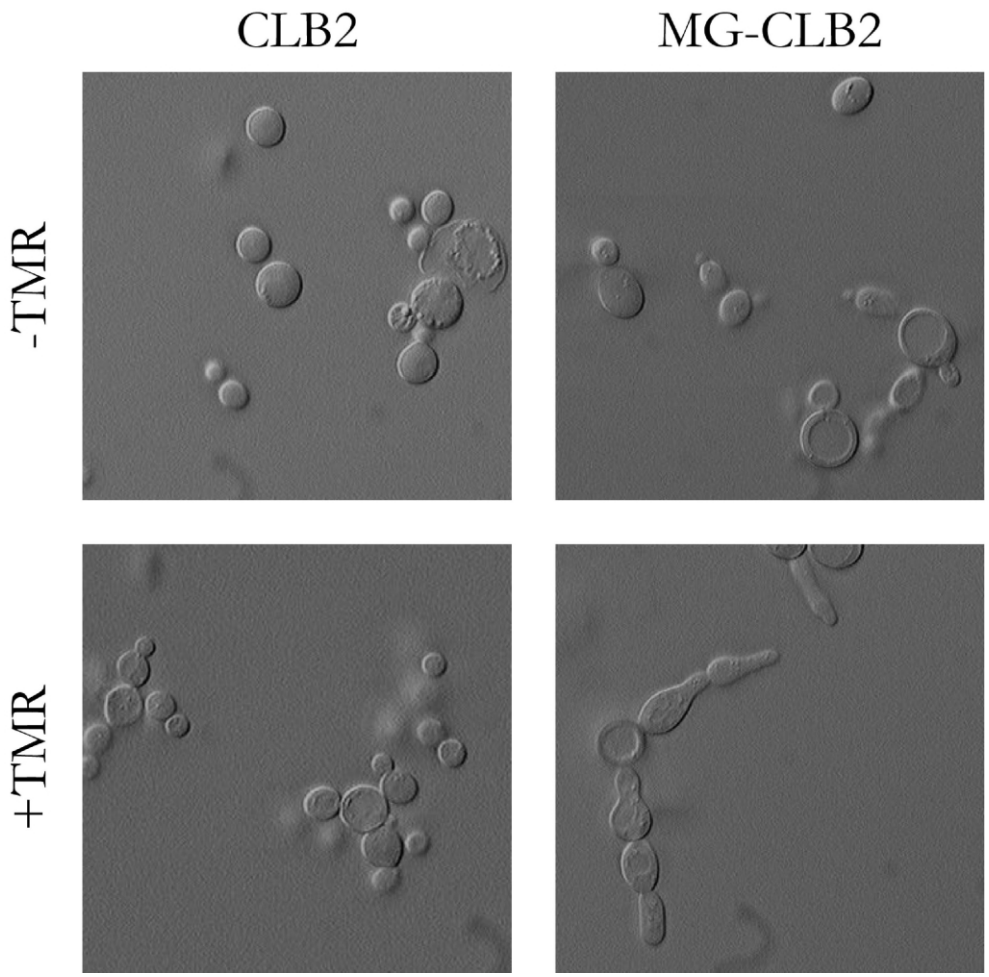

Figure 2. Log-phase control cells (*CLB2*+/clb1−/clb3−cbl4−) or aptamer-transformed cells (*MG-CLB2*/clb1−/clb3−/cbl4−) were grown in YPE media containing 2% galactose and in the absence or presence of 1 μM TMR. Cells were visualized by microscopy after 2 h.

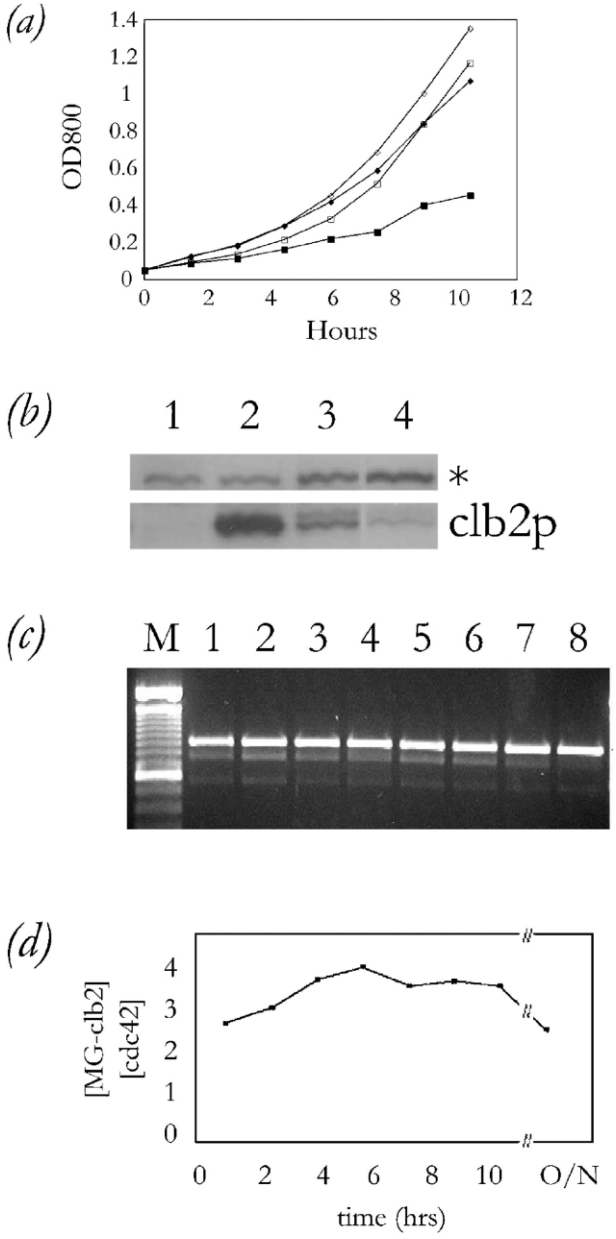

Figure 3. (a) Optical density (800 nm) was measured at fixed intervals of 90 min. Squares and circles correspond to MGClb2 and the control strain. Open and closed figures correspond to absence or presence of TMR. (b) Western analysis of Clb2 protein levels of the control and MGClb2 strains in the presence or absence of TMR. Extracts were obtained from (1) wild-type cells treated with α-factor, (2) wild-type cells treated with benomyl, (3) *MG-CLB2* cells grown without TMR, (4) *MG-CLB2* cells grown with 1 μM TMR. Anti-clb2 antibodies cross-react with an unidentified endogenous protein (marked '∗') whose concentration is invariant as a function of the cell cycle and thus serves as a convenient loading control. (c) Transcript levels were assessed by RT-PCR amplification of total RNA extracts prepared from log-phase aptamer-transformed cells at defined times before and after addition of 1 μM TMR. Primers directed to the MG aptamer itself and downstream sequence within the CLB2 open reading frame yield a diagnostic band of 777 bp. This primer set also amplifies the externally added control (*MG-CLB2*+stuffer, 934 bp). Amplification with CDC42 specific primers gives rise to a band with an approximate size of 573 bp. (M), 100 basepair marker; (1), *MG-CLB2* cells grown in the absence of TMR; (2–8), *MG-CLB2* cells grown for 1.5, 3.0, 4.5, 6.0, 7.5, 9.0, and 16 h in the presence of 1 μM TMR. (d) The ratio of *MG-CLB2*:cdc42 transcript concentration as a function of time was determined following quantitation of the bands in panel (c).

Previous studies with aptamers selected to bind FMN, ATP, citrulline, and arginine have shown that these RNAs exhibit broad (or absent) imino proton resonances and little dispersion in the absence of their ligands.[12–14] Addition of the appropriate ligand, however, causes imino proton peaks to sharpen considerably and increases dispersion in the aromatic and ribose regions of the spectra.[12–14] The malachite green aptamer structurally resembles these other aptamers in that it is composed of a conserved loop embedded within an RNA duplex. As such, we considered the possibility that ligand binding would similarly induce folding of the aptamer and might thereby account for its effect on *MG-CLB2* translation.

Figure 4 shows the results of 1-D NMR experiments on the unbound and bound forms of the MG aptamer. Five major peaks and four minor peaks are visible in the imino proton region of the spectrum in the absence of ligand. The addition of stoichiometric amounts of malachite green yields eight additional peaks. The number of imino resonances observed is close to that expected if the flanking duplexes are formed in the absence of ligand (11 peaks) and if all nucleotides within the bulge and the duplexes become structured upon addition of ligand (16 peaks). Similar changes in spectral dispersion are observed in the region 7–9 ppm where aromatic ring resonances appear. We conclude that ligand binding drives the conformation of the aptamer from an unfolded state to a folded state and speculate that this stabilization is responsible for the translational block to the *MG-CLB2* observed in the presence of malachite green.

Discussion

In vitro selection has yielded ligand-binding aptamers with affinity for ligands ranging from metal ions to proteins.[15–17] The high specificity of these molecules and the ability to automate the entire selection process has raised the possibility that aptamers may provide useful alternatives for antibodies in both therapeutic and analytical applications.[18–21] Despite extensive characterization of many selected RNAs, there remains little quantitative information on the ability of these molecules to function intracellularly (especially for aptamers that recognize small molecule ligands rather than proteins). RNAs in eukaryotic cells are generally believed to exist as complexes with non-specific RNA-binding proteins (e.g., p50, etc.) and are potential substrates for a variety of helicases that act to unwind RNA duplexes.[22,23] Association with these factors can potentially alter or inhibit the folding of aptamers to their active structures, and as such, aptamers isolated under in vitro conditions might be inactive in vivo. Using a viral expression system to overproduce intracellular transcripts, Famulok and co-workers recently demonstrated that an in vitro-evolved aptamer could specifically inhibit the activity of a transmembrane cell adhesion protein and thus block one step in a signal transduction pathway.[24] Werstuck et al. have previously shown that antibiotic and dye-binding aptamers also

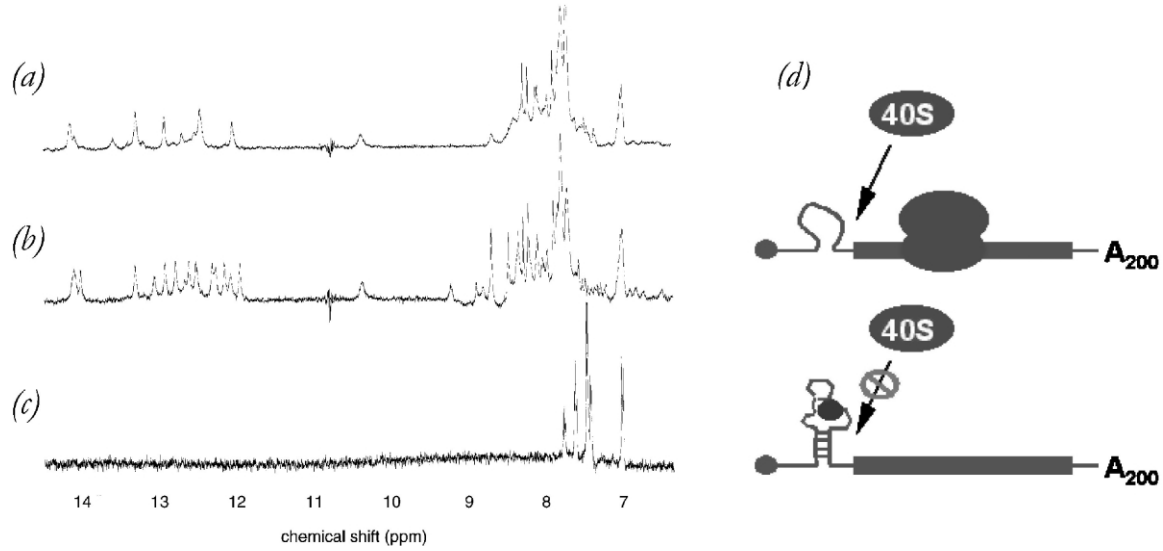

Figure 4. 1-D NMR spectra of (a) malachite green aptamer, (b) malachite green aptamer with malachite green, and (c) malachite green alone, collected as described in Experimental. Addition of malachite green yields several new sharp imino proton resonances (12–14 ppm). (d) A model for aptamer-mediated translational regulation suggested by the NMR spectra.

function in vivo.[3] The current work demonstrating activity for the malachite green aptamer provides further evidence that in vitro selected RNAs can function intracellularly.

In the current report, we show that insertion of a malachite green aptamer into the 5′-UTR of a cyclin gene transcript renders expression of the encoded protein (and thus control of the yeast cell cycle) regulated by the presence or absence of the aptamer's ligand. Our results extend upon the conceptually similar work of Werstuck et al. by directly demonstrating that ligand-mediated effects on expression do not involve changes in transcript concentration but rather transcript translatability. The presence of a single copy of the aptamer makes it possible to reduce the level of gene expression to $<10\%$ normal levels in the presence of ligand while mRNA levels remain unaffected. NMR spectroscopy demonstrates that ligand binding induces a folding transition in the aptamer, providing a physical model that can account for the change in translatability [Fig. 4(d)]. Translational initiation requires association of the 40S ribosomal subunit with the 5′-cap of an mRNA. The efficiency of this process can be modulated by the presence of structured elements near the cap (the translational apparatus of *S. cerevisiae* is especially sensitive to such structures.[1] We presume that ligand binding causes the aptamer to form a stable complex that may resist association with the ribosomal small subunit and thereby inhibit translation of the message.

Experimental

Constructs

A pRS306-derived plasmid carrying a galactose-inducible copy of *CLB2* and the URA marker (pDK29, a gift from Dr. D. Kellogg) served as the starting point for synthesis of the malachite green aptamer regulated yeast strain. Oligonucleotides corresponding to the MG aptamer sequence were chemically synthesized and ligated into the *CLB2* 5′-UTR, previously digested with Sal I and Cla I. The resulting recombinant plasmid (pDG101) was linearized and electroporated into DK162, a *CLB2*/URA-deficient strain. Transformants resulting from homologous recombination were isolated by selection on URA^- plates and then crossed with DK167, a $clb1^-/clb3^-/clb4^-$ strain. Following sporulation of diploids, tetrads were dissected and cells that grew on Leu^-/Trp^- plates were isolated. The product of these crosses yields a strain in which the endogenous *CLB2* gene and all other B-type cyclins have been knocked out and functionally replaced by *MG-CLB2*. PCR analysis using primers specific for the MG-containing form of the gene confirmed the genotype of the resulting strain.

Cell growth and preparation of cell extracts

In all reported experiments, *CLB2* and *MG-CLB2* strains were grown in shaking liquid cultures at 30 °C on YPGal media. Cell density was monitored by measuring the absorbance of cultures at 800 nm. Time points were collected at 1.5 h intervals following addition of TMR to the culture. Cell suspensions from different time points were diluted to an equivalent density with fresh media prior to analysis. Cells were pelleted and immediately frozen in liquid nitrogen. Extracts were prepared by mixing cells with lysis buffers specific for the RNA and protein quantification assays (described below), followed by vigorous vortexing with glass beads in the Vortex Genie Sleeve for 2 min.

Quantification of *CLB2* mRNA

CLB2 and *MG-CLB2* mRNA levels were measured by RT-PCR amplification of total yeast RNA. Cell extracts were prepared using a lysis buffer containing 0.3 M NaCl, 10 mM Tris (pH 7.5), 1 mM EDTA and 0.2%

SDS. Total yeast RNA was prepared by phenol-chloroform treatment of the resulting extracts. An external standard for RT-PCR was constructed by inserting a 157-bp fragment from pLG200 (a gift from S. Zaremba) into a plasmid-born copy of the MG-CLB2 gene. A mixture of 10 μg of total yeast RNA and an appropriate dilution of in vitro transcribed external standard served as template for AMV reverse transcriptase-catalyzed cDNA synthesis, primed by the *CLB2*-specific oligonucleotide 5′-GCGCAAGCTTTGGATCATTTACATCTT CTG-3′. A fraction of this reaction was amplified by PCR using the same primer and 5′-TCGAGGGATCCGC-GACTGGCGAGAGCCAGGTAACGAATCGGATCC A-3′, specific for the MG aptamer. Variation in RNA concentration between extracts was assessed by parallel RT-PCR reactions performed with primers specific for the marker CDC42 gene (5′- CGGGATCCCCAAACG CTAAAGTGTGTTG-3′ and 5′-AGCTTCTACAAAA TTGTACATTTTTTAC-3′).

Quantification of Clb2 protein

Expression of the Clb2 protein was monitored using Western blots. Extracts were prepared as described above using a sample buffer containing 60 mM Tris (pH 6.8), 2% SDS, 10% glycerol, 2 mM PMSF (phenyl methyl sulphonyl fluoride) and 1 mM LPC. Proteins were subsequently resolved by 10% Laemmli gel electrophoresis and then electrotransferred to nytran membranes. Following transfer, membranes were blocked overnight with 1X TBST (Tris-buffered saline % 0.05 Tween) containing 5% BSA and subsequently probed using 1% BSA 1X TBST with a 1/1500 dilution of primary rabbit Clb2-GST fusion antibody (obtained as previously described[25]). Following probing with the primary antibody and extensive washing with 1X TBST, anti-rabbit IgG horseradish peroxidase secondary antibody (Santa Cruz Biotech, Santa Cruz, CA) was applied at 1/1500 and 1/2000 dilutions and allowed to bind for 3 h. Following additional washing, secondary antibody binding was detected by chemiluminescence using the SuperSignal West Dura kit (Pierce, Rockford, IL) and Kodak Biomax MR film. Band intensities were quantified using the Scion Image analysis program (Scion Corp., Frederick, MD).

NMR

One-dimensional exchangeable and aromatic proton spectra were collected on a Varian 500 MHz spectrometer on samples containing 600 μM MG-aptamer RNA with or without 600 μM malachite green. RNA was resuspended in buffer containing 10 mM sodium phosphate (pH 5.8), 10 mM potassium chloride, 10 mM $MgCl_2$, and 10% D_2O. Data were collected at room temperature. Each spectrum was acquired with 128 scans and 4096 complex points. During data acquisition, water suppression was achieved by pre-irradiation of the water signal.

Acknowledgements

The authors wish to thank Jim Loo for NMR spectra collection, Dr. Kellogg for technical assistance and Drs. Kellogg and Ares for advice. Supported by awards to C.W. from the NIH, NSF, and David and Lucile Packard Foundation.

References

1. Kozak, M. *J. Biol. Chem.* **1991**, *266*, 19867.
2. Sachs, A. B.; Sarnow, P.; Hentze, M. W. *Cell* **1997**, *89*, 831.
3. Werstuck, G.; Green, M. R. *Science* **1998**, *282*, 296.
4. Futcher, A. B. *Semin. Cell Biol.* **1991**, *2*, 205.
5. Bragulat, M. R.; Abarca, M. L.; Castellá, G.; Cabañes, F. *J. Appl. Bacteriol.* **1995**, *79*, 578.
6. Elliot, A.; Morgan, U. M.; Thompson, R. C. A. *J. Gen. Appl. Microbiol.* **1999**, *45*, 139.
7. Golding, P. S.; King, T. A.; Maddocks, L.; Drucker, D. B.; Blinkhorn, A. S. *J. Photochem. Photobiol. B—Biol.* **1998**, *47*, 202.
8. Baugh, C.; Grate, D.; Wilson, C. *J. Mol. Biol.* **2000**, *301*, 117.
9. Chen, C. Y.; Xu, N.; Shyu, A. B. *Mol. Cell. Biol.* **1995**, *15*, 5777.
10. Chant, J. *Annu. Rev. Cell Dev. Biol.* **1999**, *15*, 365.
11. Hermann, T.; Patel, D. J. *Science* **2000**, *287*, 820.
12. Dieckmann, T.; Suzuki, E.; Nakamura, G. K.; Feigon, J. *Rna* **1996**, *2*, 628.
13. Fan, P.; Suri, A. K.; Fiala, R.; Live, D.; Patel, D. J. *J. Mol. Biol.* **1996**, *258*, 480.
14. Yang, Y.; Kochoyan, M.; Burgstaller, P.; Westhof, E.; Famulok, M. *Science* **1996**, *272*, 1343.
15. Tuerk, C.; Gold, L. *Science* **1990**, *249*, 505.
16. Ciesiolka, J.; Gorski, J.; Yarus, M. *Rna* **1995**, *1*, 538.
17. Binkley, J.; Allen, P.; Brown, D. M.; Green, L.; Tuerk, C.; Gold, L. *Nucleic Acids Res.* **1995**, *23*, 3198.
18. Pagratis, N. C.; Bell, C.; Chang, Y. F.; Jennings, S.; Fitzwater, T.; Jellinek, D.; Dang, C. *Nat. Biotechnol.* **1997**, *15*, 68.
19. Bock, L. C.; Griffin, L. C.; Latham, J. A.; Vermaas, E. H.; Toole, J. J. *Nature* **1992**, *355*, 564.
20. Hamasaki, K.; Killian, J.; Cho, J.; Rando, R. R. *Biochemistry* **1998**, *37*, 656.
21. Kubik, M. F.; Bell, C.; Fitzwater, T.; Watson, S. R.; Tasset, D. M. *J. Immunol.* **1997**, *159*, 259.
22. Iost, I.; Dreyfus, M.; Linder, P. *J. Biol. Chem.* **1999**, *274*, 17677.
23. de la Cruz, J.; Kressler, D.; Linder, P. *Trends Biochem. Sci.* **1999**, *24*, 192.
24. Blind, M.; Kolanus, W.; Famulok, M. *Proc. Natl. Acad. Sci. U.S.A.* **1995**, *96*, 3606.
25. Kellog, D. R.; Murray, A. W. *J. Cell Biol.* **1999**, *130*, 675.